Monodisperse Thioether-Stabilized Palladium Nanoparticles: Synthesis, Characterization, and Reactivity

Mani Ganesan, Ruel G. Freemantle, and Sherine O. Obare*

Department of Chemistry, Western Michigan University, Kalamazoo, Michigan 49008

Received November 8, 2006. Revised Manuscript Received April 12, 2007

Size control of monodisperse palladium nanoparticles with sizes ranging from 1.7 to 3.5 nm was accomplished using thioethers as stabilizing ligands, in a one-step procedure. Modulation of the reaction temperature, reaction time, solvent, and carbon chain length of the thioether provided control over the nanoparticle size and size distribution. The resulting Pd nanoparticles were characterized by transmission electron microscopy (TEM), high-resolution transmission electron microscopy (HRTEM), and X-ray diffraction (XRD). ^{1}H NMR spectroscopy provided insight into the thioether−Pd nanoparticle surface interaction. To demonstrate the catalytic activity of the thioether-stabilized Pd nanoparticles, hydrogenation reactions were carried out using the as-synthesized Pd nanoparticles. We observed a trend in the reactivity of the nanoparticles with respect to their size, however, recovery of the nanoparticles following subsequent reactions was rather challenging. Immobilization of the Pd nanoparticles onto commercial SiO_2 resulted in rapid and efficient catalysis, successful recovery of the Pd nanoparticles, and furthermore, the nanoparticles could be used up to 8 times with no measurable decrease in catalytic activity. This work demonstrates the utility of thioether ligands for the synthesis of monodisperse Pd nanoparticles that are efficient catalysts for various organic transformations.

Introduction

Metal nanoparticles continue to attract interest because of their unusual properties and potential applications in catalysis, sensing, magnetics, optics, and electronics. The preparation of uniform palladium nanoparticles has been intensively pursued because of their applications as catalysts in organic transformations, for example, carbon−carbon coupling reactions[1] and olefin hydrogenation reactions.[2] A major challenge exists in the ability to produce well-defined and monodisperse Pd nanoparticles in the 1−4 nm size range, where high surface-to-volume ratio and increase in surface atom distribution greatly enhance the catalytic activity. Several procedures have been reported that produce Pd nanoparticles,[3] but notably, only few of these procedures yield monodisperse Pd nanoparticles. Despite these efforts, there is need for straightforward and reliable methods that produce large quantities of uniform, stable, and monodisperse Pd nanoparticles in the desired size range. Typical stabilizing ligands reported for Pd nanoparticle stabilization include dendrimers,[4] phosphine ligands,[3a−b] thiols,[5] and polymers.[6]

Here, we report the use of thioether ligands to synthesize stable and monodisperse Pd nanoparticles with sizes of 1.7 ± 0.2 nm, 1.9 ± 0.2 nm, 2.5 ± 0.1 nm, 3.5 ± 0.1 nm, and 4.1 ± 0.1 nm by either a one-step (1) pyrolysis, (2) polyol reduction, or (3) a room-temperature chemical reduction method. Surprisingly, thioethers have not been fully exploited as metal nanoparticle stabilizers or in the control of particle size. With the exception of work reported by Hussain et al., little has been done in the area of thioether-stabilized metal nanoparticles.[7] Thioethers mimic phosphine ligands as being

* To whom correspondence should be addressed. Tel: 269-387-2923. Fax: 269-387-2909. E-mail: sherine.obare@wmich.edu.

(1) (a) Narayanan, R.; El-Sayed, M. A. *J. Phys. Chem. B* **2004**, *108*, 8572−8580. (b) Pittelkow, M.; Moth-Poulsen, K.; Boas, U.; Christensen, J. *Langmuir* **2003**, *19*, 7682−7684. (c) Li, Y.; El-Sayed, M. A. *J. Phys. Chem. B* **2001**, *105*, 8938−8943. (d) Yeung, L. K.; Crooks, R. M. *Nano Lett.* **2001**, *1*, 14−17. (e) Yeung, L. K.; Lee, C. T.; Johnston, K. P.; Crooks, R. M. *Chem. Commun.* **2001**, 2290−2291. (f) Ooe, M.; Murata, M.; Mizugaki, T.; Ebitani, K.; Kaneda, K. *J. Am. Chem. Soc.* **2004**, *126*, 1604−1605. (g) Rahim, E. H.; Kamounah, F. S.; Frederiksen, J.; Christensen, J. B. *Nano Lett.* **2001**, *1*, 499−501.

(2) (a) Zhao, M.; Crooks, R. M. *Angew. Chem., Int. Ed.* **2000**, *39*, 165. (b) Crooks, R. M.; Zhao, M.; Sun, L.; Chechik, V.; Yeung, L. K. *Acc. Chem. Res.* **2001**, *34*, 181.

(3) (a) Chen, M.; Falkner, J.; Guo, W.−H.; Zhang, J.−Y.; Sayes, C.; Colvin, V. L. *J. Colloid Interface Sci.* **2005**, *287*, 146−151. (b) Kim, S.−W.; Park, J.; Jang, Y.; Chung, Y.; Hwang, S.; Hyeon, T. *Nano. Lett.* **2003**, *3*, 1289−1291. (c) Son, S. U.; Jang, Y.; Yoon, K. Y.; Kang, E.; Hyeon, T. *Nano Lett.* **2004**, *4*, 1147−1151. (d) Zhao, M.; Sun, L.; Crooks, R. M. *J. Am. Chem. Soc.* **1998**, *120*, 4877−4878. (e) Zhao, M.; Crooks, R. M. *Angew. Chem., Int. Ed.* **1999**, *38*, 364−366. (f) Niu, Y.; Yeung, L. K.; Crooks, R. M. *J. Am. Chem. Soc.* **2001**, *123*, 6840−6846. (g) Garcia-Martinez, J. C.; Scott, R. W. J.; Crooks, R. M. *J. Am. Chem. Soc.* **2003**, *125*, 11190−11191.

(4) (a) Oh, S. K.; Niu, Y. H.; Crooks, R. M. *Langmuir* **2005**, *21*, 10209−10213. (b) Jiang, G. H.; Wang, L.; Chen, T.; Yu, H. J.; Wang, J. J. *Nanotechnology* **2004**, *15*, 1716−1719. (c) Ye, H. C.; Scott, R. W. J.; Crooks, R. M. *Langmuir* **2004**, *20*, 2915−2920. (d) Oh, S. K.; Kim, Y. G.; Ye, H. C.; Crooks, R. M. *Langmuir* **2003**, *19*, 10420−10425. (e) Scott, R. W. J.; Ye, H. C.; Henriquez, R. R.; Crooks, R. M. *Chem. Mater.* **2003**, *15*, 3873−3878. (f) Niu, Y. H.; Crooks, R. M. *Chem. Mater.* **2003**, *15*, 3463−3467.

(5) (a) Zelakiewicz, B. S.; Lica, G. C.; Deacon, M. L.; Tong, Y. *J. Am. Chem. Soc.* **2004**, *126*, 10053−10058. (b) Chen, S.; Huang, K.; Stearns, J. *Chem. Mater.* **2000**, *12*, 540−547. (c) Yee, C. K.; Jordan, R.; Ulman, A.; White, H.; King, A.; Rafailovich, M.; Sokolov, J. *Langmuir* **1999**, *15*, 3486−3491.

(6) (a) Narayanan, R.; El-Sayed, M. A. *J. Phys. Chem. B* **2004**, *108*, 8572−8580. (b) Narayanan, R.; El-Sayed, M. A. *J. Am. Chem. Soc.* **2003**, *125*, 8340−8347. (c) Cioffi, N.; Torsi, L.; Losito, I. *Electrochim. Acta* **2001**, *46*, 4205−4211. (d) Wang, J. G.; Neoh, K. G.; Kang, E. T. *J. Colloid Interface Sci.* **2001**, *239*, 78−86.

(7) Hussain, I.; Graham, S.; Wang, Z.; Tan, B.; Sherrington, D. C.; Rannard, S. P.; Cooper, A. I.; Burst, M. *J. Am. Chem. Soc.* **2005**, *127*, 16398−16399.

10.1021/cm062655q CCC: $37.00
Published on Web 06/07/2007

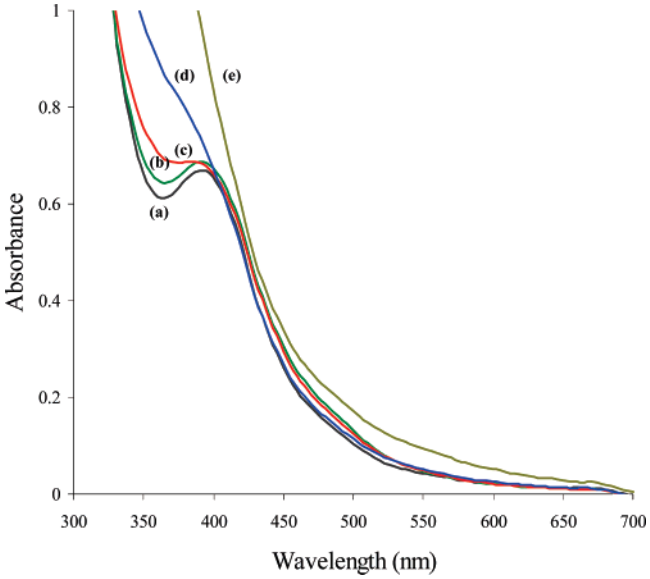

Figure 1. UV−vis absorbance spectra of $[Pd_3(OAc)_6]$ and *n*-dodecyl sulfide in a 1:5 ratio, respectively, dissolved in toluene. As the temperature is raised from room temperature to 95 °C, Pd nanoparticles begin to form, and the color of the solution changes from yellow to dark brown. At 80 °C, the solution color is completely dark brown indicating formation of Pd nanoparticles. (a) 0 min, (b) 10 min, (c) 20 min, (d) 30 min, and (e) 40 min. No change in UV−vis absorbance spectra was observed following 40 min, indicating Pd nanoparticle formation.

soft donors but are less toxic and are relatively easy to handle in air. We have investigated the use of several thioether ligands and have observed particle size variations with respect to temperature, duration of heating, and thioether carbon chain length. The Pd nanoparticles were effective in the hydrogenation of olefins under both homogeneous and heterogeneous conditions.

Experimental Procedures

Materials. Palladium acetate $[Pd_3(OAc)_6]$ (OAc = acetate), palladium chloride, ethyl sulfide, propyl sulfide, butyl sulfide, hexyl sulfide, *n*-dodecyl sulfide, silica gel 200−400 mesh, hydrazine hydrate, sodium hydroxide, sodium chloride, and sodium were purchased from Aldrich Chemicals and were used with no further purification. Bis(11-carboxyundecyl) sulfide was prepared following a literature procedure.[8] All solvents (Aldrich Chemicals) were of HPLC grade or better and were distilled prior to use. All Pd nanoparticles were prepared following standard Schlenk line techniques.

Instrumentation. A JEOL electron microscope, Model JEM-1230, was used to obtain transmission electron microscope (TEM) images. A JEOL 3011 high-resolution transmission electron microscope (HRTEM) was used for high resolution and electron diffraction measurements. Powder X-ray diffraction (XRD) data was collected on a Scintag XDS Model 2000 diffractometer. For XRD measurements, the Pd nanoparticle sample was dried and mixed with 325 mesh Si powder and was placed on a Si wafer sample holder. Gas chromatography mass spectrometry data were collected using a Hewlett-Packard HP 6890 Series instrument. A JEOL Eclipse 400 MHz NMR spectrometer was used to acquire ^1H NMR spectra. Chemical shifts (δ) were referenced to signals due to residual protons present in the deuterated toluene-d_8 solvent. UV−vis absorption spectra were acquired using a Varian Cary 50 spectrophotometer.

Synthesis of Pd Nanoparticles from $[Pd_3(OAc)_6]$ by Pyrolysis. Palladium acetate $[Pd_3(OAc)_6]$ (0.20 g, 0.30 mmol) and *n*-dodecyl sulfide (1.65 g, 4.45 mmol) were added to 50 mL of toluene. The resulting solution was heated to 95 °C and remained at this temperature for 3 h. The color of the solution turned from orange to black. The solvent was removed under vacuum, and the resultant residue was washed with acetone (25 mL) twice and then centrifuged resulting in 3.5 nm Pd nanoparticles. Similar reactions were carried out using ethyl sulfide, propyl sulfide, butyl sulfide, hexyl sulfide, and octyl sulfide at 95 °C in toluene for 1 h.

Synthesis of Pd Nanoparticles from $[PdCl_4]Na_2$ by Hydrazine Reduction. A solution of $[PdCl_4]Na_2$ (0.011 M) in ethanol (250 mL) was prepared by the reaction of $PdCl_2$ (0.500 g, 2.82 mmol) and NaCl (0.33 g, 5.64 mmol) at room temperature. To an ethanol (40 mL) solution of *n*-dodecyl sulfide (0.203 g, 0.55 mmol), $[PdCl_4]Na_2$ (10 mL, 0.11 mmol) was added to form a yellow-colored solution. To this solution, a mixture of hydrazine hydrate (0.011 mL, 0.22 mmol) and sodium hydroxide (0.43 mL, 0.51 M, 0.22 mmol) in ethanol (10 mL) was rapidly added, and the solution color changed immediately to black. The resulting solution was left undisturbed for about 30 min and was followed by centrifugation, which provided dark Pd nanoparticles. The Pd nanoparticles were redispersed into toluene and were analyzed by TEM.

Place Exchange Reactions. Exchange of *n*-dodecyl sulfide ligands from the Pd nanoparticle surface was demonstrated by a place exchange reaction with the sodium salt of bis(11-carboxyundecyl) sulfide. A solution of the sodium salt of bis(11-carboxyundecyl) sulfide was prepared by the reaction of bis(11-carboxyundecyl) sulfide (0.059 g, 146 mmol) and NaOH (0.051 M, 0.57 mL) in water (20 mL). A toluene solution of Pd nanoparticles prepared by diluting the *n*-dodecyl sulfide stabilized Pd nanoparticles (2 mL) obtained from the pyrolysis reaction described above with toluene (20 mL) was added to form an immiscible layer above the aqueous bis(11-carboxyundecyl) sulfide layer. The mixture was stirred for 5 min after which the bottom aqueous layer was dark and the top toluene layer was colorless, indicating that the Pd nanoparticles were in the aqueous layer. The aqueous layer was analyzed by TEM and showed discrete monodisperse Pd nanoparticles. The Pd nanoparticles were stable in aqueous solution for at least 7 days.

General Method for Styrene Hydrogenation using Pd Nanoparticles. The flask was connected to vacuum for a few seconds then connected to a rubber bladder containing H_2 (~1 atm) and was stirred at room temperature for the required time. Pd nanoparticles of 1.7 ± 0.2 nm, 2.5 nm ± 0.1 nm, and 3.5 ± 0.1 nm were prepared by pyrolysis as described above. The 0.5 mL (3 mmol) of each of the Pd nanoparticles was allowed to react with styrene (5 mL, 43.5 mmol). The resultant solution was refluxed for 1 h, and analysis of an aliquot of the solution by gas chromatography−mass spectrometry (GC-MS) showed complete conversion of styrene to ethylbenzene. Following each reaction, nanoparticle recovery became problematic, and a majority of the nanoparticles aggregated. In addition, the catalyst reactivity decreased significantly after the first cycle.

General Method for the Immobilization of Pd Nanoparticles on Silica To Form Pd/SiO_2. Prior to Pd nanoparticle immobilization, silica gel was heated at 400 °C in an oven for 5 h and was cooled to room temperature under vacuum. Generally, the immobilization of Pd nanoparticles onto SiO_2 proceeded as follows: an appropriate quantity of silica gel was taken in a 200 mL Schlenk flask and was connected to a manifold Schlenk line, containing benzene or toluene (50 mL). The as-synthesized Pd nanoparticles (2 mL, ca. 0.012 mmol, produced from the pyrolysis reaction

(8) Troughton, E. B.; Bain, C. D.; Whitesides, G. M.; Nuzzo, R. G.; Allara, D. L.; Porter, M. D. *Langmuir* **1998**, *4*, 365−385.

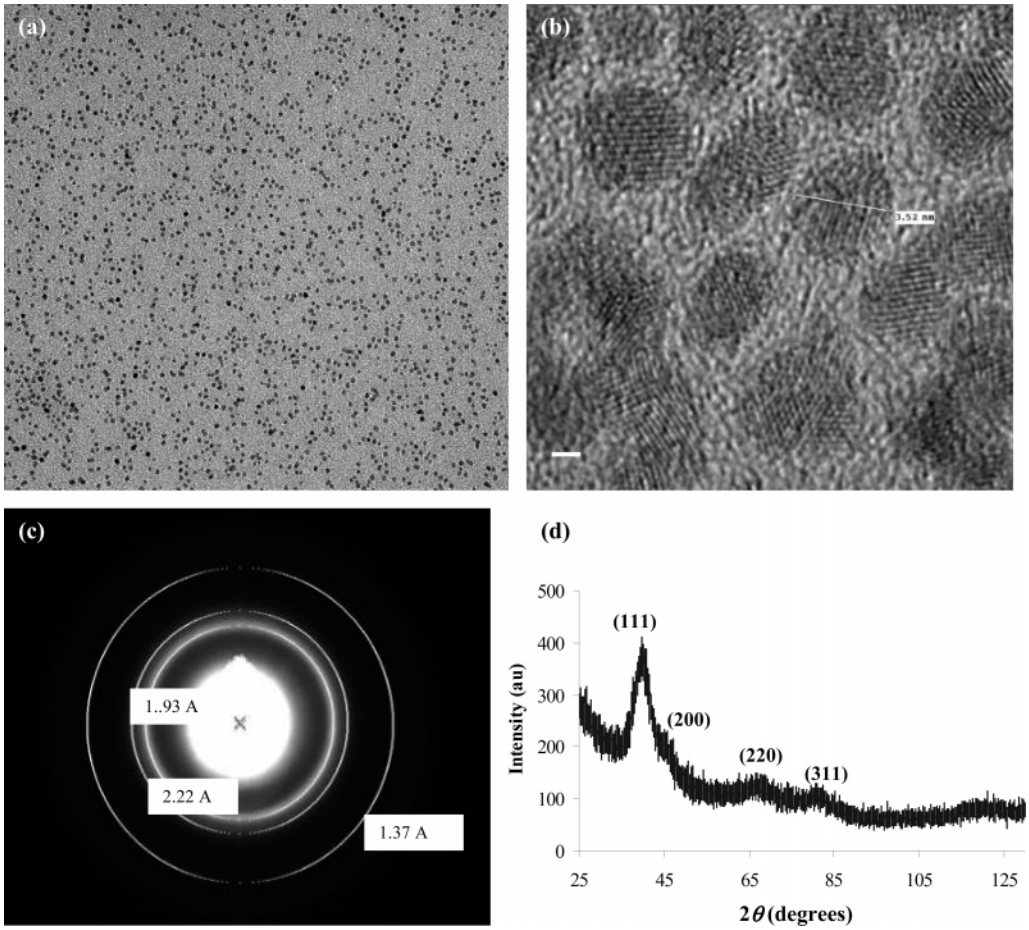

Figure 2. TEM image of 3.5 nm palladium nanoparticles synthesized by thermal decomposition of $Pd(OAc)_2$ in toluene, using *n*-dodecyl sulfide; scale bar = 50 nm. The inset shows the corresponding size distribution obtained by counting 100 randomly selected particles. (b) HRTEM image of 3.5 nm *n*-dodecyl sulfide stabilized palladium nanoparticles; scale bar = 1 nm. (c) Electron diffraction image of a single Pd nanoparticle exhibiting three diffused rings which could be assigned to the {111}, {220}, and {311} reflections. (d) XRD patterns of Pd nanoparticles with average size of 3.5 nm.

described above) were slowly added to the contents of the flask and were stirred for 5 min. The color of the silica gel turned dark while the supernatant solution became colorless, indicating that the Pd nanoparticles were immobilized on SiO_2. The supernatant solution was decanted and the slurry was washed with benzene or toluene three times to remove excess *n*-dodecyl sulfide.

General Method for Hydrogenation Reactions Using Pd/SiO_2. Benzene or toluene (50 mL) was added to the 2 g of the Pd/SiO_2 catalyst, followed by addition of an appropriate amount of either styrene (2 mL, 17.40 mmol), 1,5-cyclooctadiene (1 mL, 8.15 mmol), or 6-bromo-1-hexene (0.2 mL, 1.50 mmol), on the basis of the hydrogenation reaction carried out. The flask was connected to vacuum for a few seconds then connected to a rubber bladder containing H_2 (~1 atm) and was stirred at room temperature for the required time. After the experiment was complete, the supernatant solution was decanted, the flask was recharged with the appropriate quantities of the reactants, and then the experiment was repeated as before.

Results and Discussion

Fabrication, Size Control, and Characterization of Pd Nanoparticles. Monodisperse thioether-stabilized Pd nanoparticles were generated in gram scale by pyrolysis. A typical synthetic procedure involved the pyrolysis of $[Pd_3(OAc)_6]$ in the presence of *n*-dodecyl sulfide (M:L = 1:5) in toluene at 95 °C for 3 h. Within 25 min and at a temperature of 90 °C, the color of the reaction turned from yellow to black and the UV−vis absorbance spectrum showed disappearance of the 400 nm peak corresponding to a toluene solution of $[Pd_3(OAc)_6]$, as shown in Figure 1. The darkening of the solution indicated colloidal Pd nanoparticle formation. On the basis of Pd content, the concentration of the solution was 0.006 M. Pyrolysis of $[Pd_3(OAc)_6]$ in toluene in the absence of *n*-dodecyl sulfide did not produce a dark colloidal solution. The as-synthesized Pd nanoparticles were monodisperse and measured 3.5 ± 0.1 nm in diameter, as shown in Figure 2a, which was obtained with no size selection process. The nanoparticles adopted a spherical shape indicating isotropic growth. These Pd nanoparticles could be redispersed into hexane, toluene, or THF solvents and the solutions were stable in air for days. Pd nanoparticles produced from reactions where the Pd:L (where L = *n*-dodecyl sulfide) was 3:1, 4:1, 5:1, or higher showed significant control over the nanoparticle size and size distribution. However, with Pd:L ratios less than 3:1, the Pd nanoparticles formed were insoluble because of insufficient amount of the stabilizing ligand. HRTEM showed twinning of the Pd nanoparticles, which is typical of most metal nanoparticles as shown in Figure 2b.[9] The electron diffraction image of ~3.5 nm

(9) Sampedro, B.; Crespo, P.; Hernando, A.; Litran, R.; Lopez, J. C. S.; Cartes, C. L.; Fernandez, A.; Ramirez, J.; Calbet, J. G.; Vallet, M. *Phys. Rev. Lett.* **2003**, *91*, 237203-1−237203-4.

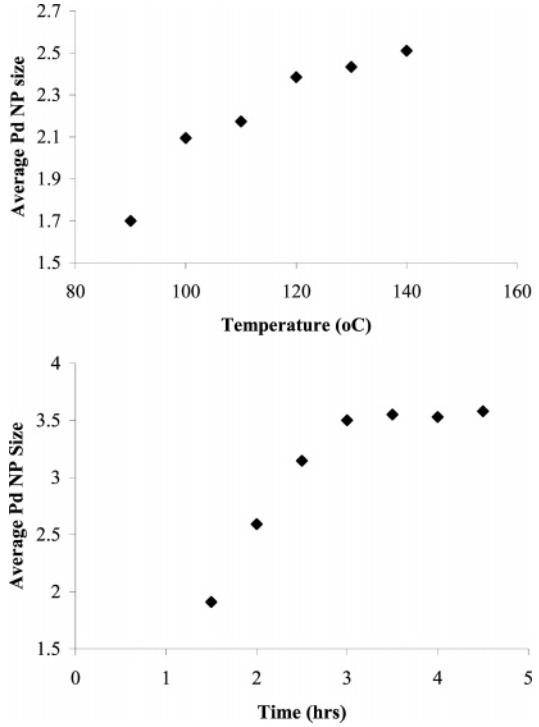

Figure 3. Plot of (a) average Pd nanoparticle size vs temperature; increase in temperature results in an increase in nanoparticle size until ~140 °C, and (b) average nanoparticle size vs increase in reaction time at 95 °C demonstrates that for reaction time up to 3 h, the particles continue to grow, but after 3 h no further growth occurs.

Pd nanoparticles exhibited three diffused rings which could be assigned to the {111}, {220}, and {311} reflections of a face-centered cubic Pd (Figure 2c). XRD measurements showed a broad peak at 40 degrees, characteristic of the (111) peak of zerovalent Pd with face-centered cubic (fcc) structure as shown in Figure 2d. Nanoparticle size was calculated from the line broadening of (111) reflection using the Sherrer's formula and showed an average nanoparticle size of ~3 nm. It is well-known that thioethers bind to metal surfaces through a dative bond.[10] The ^{1}H NMR spectrum of the *n*-dodecyl sulfide stabilized Pd nanoparticles showed broad peaks for the methylene and methyl groups, suggesting that the ligand was coordinated to the Pd nanoparticles.

Modulation of reaction conditions during nanoparticle synthesis plays a significant role in controlling the size and shape of the particles. We investigated the effects of (1) reaction temperature and (2) reaction time on the pyrolysis of $[Pd_3(OAc)_6]$. Both conditions were found to have a profound influence on the nanoparticle size as well as on the size distribution. One hour pyrolysis of a toluene solution containing a 1:5 ratio of $[Pd_3(OAc)_6]$ to *n*-dodecyl sulfide was carried out at temperatures of 95, 100, 110, 120, 130, and 140 °C, yielding in each case monodisperse Pd nanoparticles with sizes of 1.7 ± 0.2 nm, 2.1 ± 0.2 nm, 2.2 ± 0.2 nm, 2.3 ± 0.1 2.4 ± 0.1 nm, and 2.5 ± 0.1 nm, respectively. The graph in Figure 3a shows the effect of temperature on Pd nanoparticle growth. We found that increasing the reaction temperature resulted in an increase in particle size, accompanied by a narrower size distribution. In addition, the effect of reaction heating time was investigated. Figure 3b shows a plot of nanoparticles size as a function of reaction time. The data reveals that the average Pd nanoparticles size increase from 0 to 3 h and then levels off. This is consistent with Ostwald ripening during the first 3 h, which levels off because of depletion of smaller Pd nanoparticles, as well as any free Pd atoms that may be present in solution. A representation of the size control and narrow size distribution of the synthesized nanoparticles is shown in Figure 4a−d, demonstrating the ability to fine-tune the particle size by controlled reaction time. Furthermore, prolonged reaction time resulted in larger size distributions. Both results indicate that particle growth is consistent with an Ostwald ripening procedure, whereby prolonged reflux time or heating time results in nanoparticles with larger diameters.[11]

The effect of thioether chain length on the Pd nanoparticle dispersity was also studied. Pyrolysis reactions of toluene solutions containing $[Pd_3(OAc)_6]$ and either ethyl sulfide, propyl sulfide, butyl sulfide, hexyl sulfide, or octyl sulfide in a 1:5 ratio were carried out at 95 °C for 1 h and were compared to the reactions with *n*-dodecyl sulfide. TEM images of the resulting Pd nanoparticles are shown in Figure 5a−f. The images show that Pd nanoparticles are formed with shorter chain thioethers, however, the particles are polydisperse and range in size from 1.5 to 7.3 nm in diameter for up to six carbon chains. Above six carbon chains, the particles have a narrower size distribution as shown in Figure 5e and 5f for octyl sulfide and *n*-dodecyl-sulfide, respectively. Longer reaction times (3 h) at 95 °C for these shorter chain sulfide ligands resulted in larger nanoparticles that were also polydisperse and ranged in diameter from 1.5 to 20 nm.

Polyol reduction of $[Pd_3(OAc)_6]$ in the presence of *n*-dodecyl sulfide yielded monodisperse 1.7 ± 0.2 nm Pd nanoparticles. Briefly, $[Pd_3(OAc)_6]$ and *n*-dodecyl sulfide in a Pd:L = 1:5 molar ratio were dissolved in ethanol and were heated at 50 °C for 1 h resulting in a dark colloidal solution consisting of Pd nanoparticles. When the same reaction was carried out using toluene as solvent instead of ethanol, the Pd colloids did not form. Palladium acetate in the presence of thioethers is known to activate C−H bonds,[12] and therefore toluene is both a solvent as well as a reactant.[13] That colloidal Pd nanoparticles formed from $[Pd_3(OAc)_6]$ in toluene only when the temperature was raised to 95 °C and not at 50 °C as in the case of ethanol prompted us to confirm that ethanol was involved in the reduction process. Toshima et al.[14] and Chen et al.[15] have independently shown that alcohols such as ethanol reduce Pd(II) complexes and produce nanoscale Pd particles. When $[PdCl_4]Na_2$ was used instead of $[Pd_3(OAc)_6]$ in the presence of *n*-dodecyl sulfide in ethanol and

(10) Love, J. C.; Estroff, L. A.; Kriebel, J. K.; Nuzzo, R. G.; Whitesides, G. M. *Chem. Rev.* **2005**, *105*, 1103−1169.

(11) (a) Ostwald, W. *Z. Phys. Chem.* **1901**, *37*, 385. (b) Voorhees, P. W. *J. Stat. Phys.* **1985**, *38*, 231.

(12) Fuchita, Y.; Hiraki, K.; Kamogawa, Y.; Suenaga, M. *J. Chem. Soc., Chem. Commun.* **1987**, 941−942.

(13) ^{1}H NMR spectra of the Pd nanoparticles formed in toluene showed the presence of biphenyl derivatives, which we attribute as being due to C−H activation by the palladium acetate−*n*-dodecyl sulfide. GC-MS data further supported the presence of the biphenyl derivatives.

(14) Toshima, N.; Shiraishi, Y.; Teranishi, T.; Miyake, M.; Tominaga, T.; Watanabe, H.; Brijoux, W.; Bonnemann, H.; Schmid, G. *Appl. Organometal. Chem.* **2001**, *15*, 178−196.

(15) Chen, F.; Zhong, Z.; Xu, X.-J.; Luo, J. *J. Mater. Sci.* **2005**, *40*, 1517−1519.

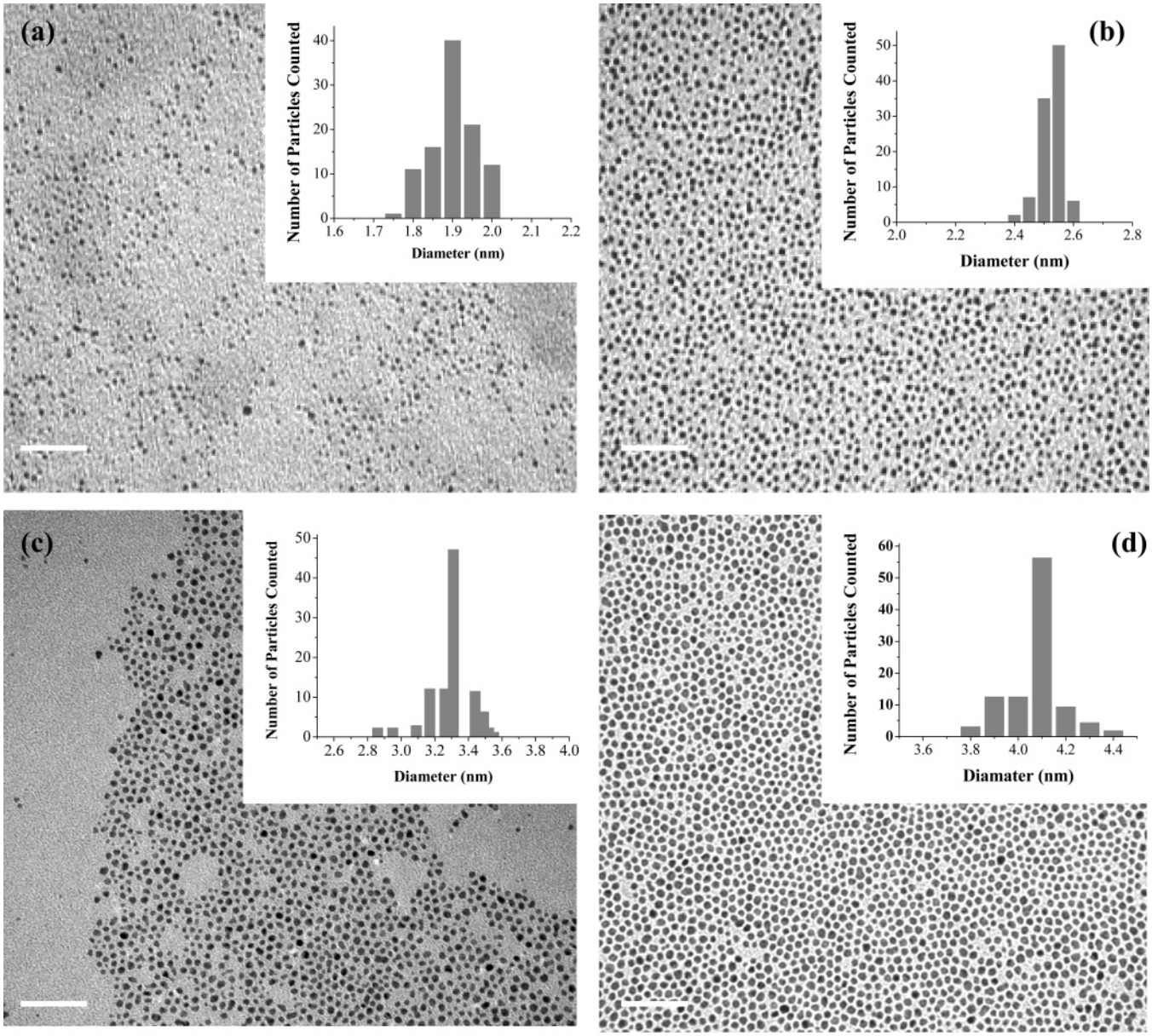

Figure 4. Transmission electron micrographs and size distribution histograms (insets) for *n*-dodecyl-sulfide stabilized palladium nanoparticles: (a) 1.9 ± 0.2 nm, (b) 2.5 ± 0.1 nm, (c) 3.3 ± 0.1 nm, and (d) 4.1 ± 0.1 nm. All images were acquired without a size selection process. Scale bar = 50 nm.

refluxed, surprisingly, no colloidal Pd nanoparticles formed. This suggested that ethanol may only be partially involved in the reduction process and that the acetate ligand (OAc^-) contributes to the reduction of Pd^{2+} to Pd^0. Indeed, Yee et al.[16] showed the generation of Pd nanoparticles by pyrolysis of palladium acetate or palladium chloride and sodium acetate, whereby the acetate radical formed in the reaction was suggested to assist in $Pd^{2+} \rightarrow Pd^0$ reduction. The results suggest two possibilities, either (1) the complex formed between $PdCl_4[Na]_2$ and *n*-dodecyl has a higher reduction potential than the complex formed between $Pd_3(OAc)_6$ and *n*-dodecyl sulfide, or (2) that a synergy between ethanol and the acetate ion exists that allows Pd nanoparticles to form in ethanol under milder conditions than in toluene. The mechanism is currently being further investigated.

Alternative to thermal decomposition, monodisperse Pd nanoparticles were synthesized by chemical reduction of $[PdCl_4]Na_2$ with hydrazine hydrate in the presence of NaOH using *n*-dodecyl sulfide as a stabilizing ligand at room temperature in ethanol. The resulting Pd nanoparticles were centrifuged and dispersed in toluene. TEM analysis showed that the Pd nanoparticles were monodisperse with a diameter of 3.5 ± 0.1 nm.

Ligands that effectively control nanoparticle size and stabilize the surface, but allow easy exchange with other ligands, are important in colloidal chemistry. *n*-Dodecyl sulfide stabilized Pd nanoparticles in toluene were exchanged with bis(11-carboxyundecyl) sulfide in water by a place exchange reaction. The bis(11-carboxyundecyl) sulfide stabilized Pd nanoparticles were analyzed by TEM, which showed discrete Pd nanoparticles with no signs of aggregation. The nanoparticles were stable in water for days.

(16) Yee, C. K.; Jordan, R.; Ulman, A.; White, H.; King, A.; Rafailovich, M.; Sokolov, J. *Langmuir* **1999**, *15*, 3486−3491.

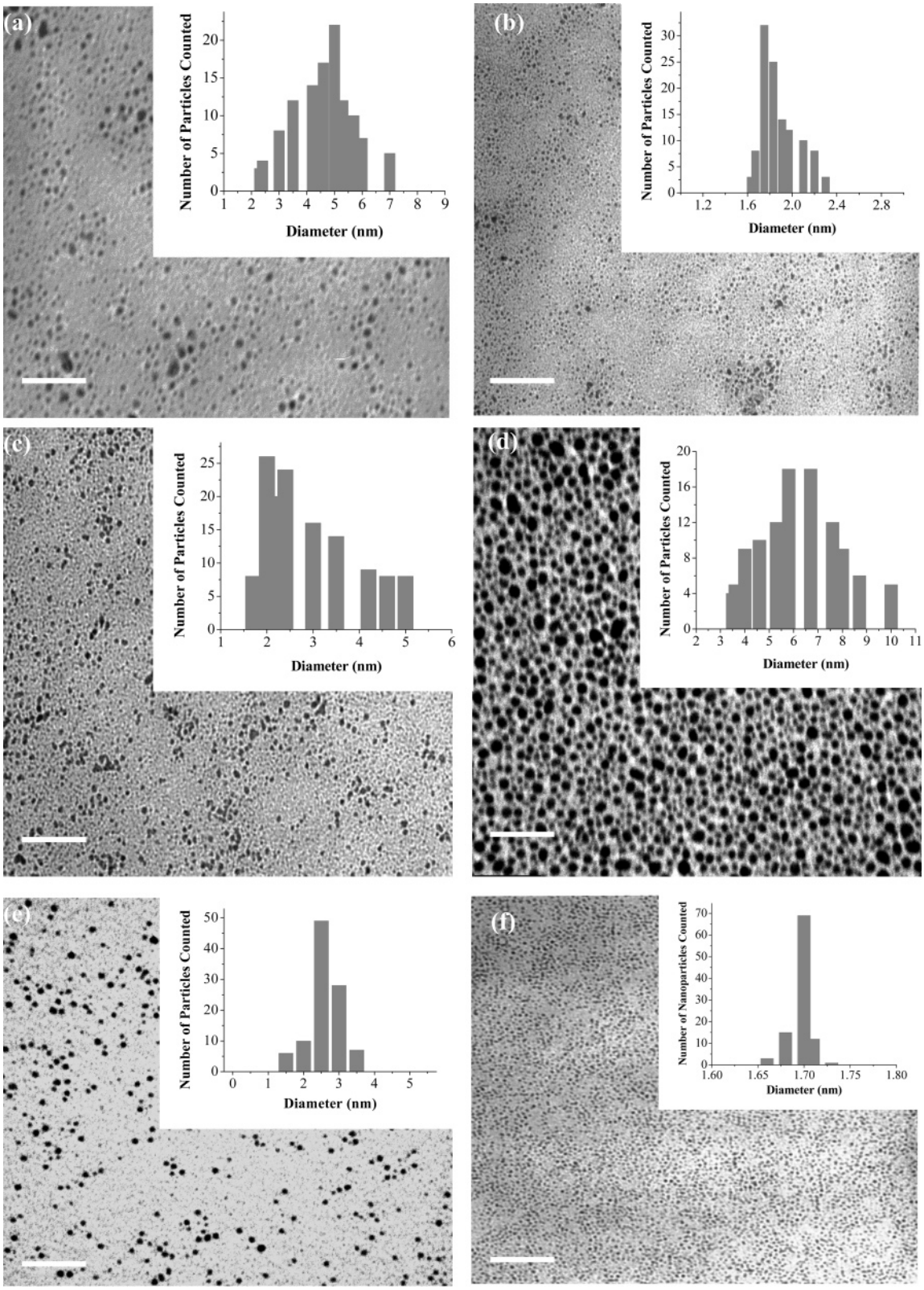

Figure 5. TEM images of Pd nanoparticles and their corresponding size histograms (inset), obtained by 1 h pyrolysis reactions in toluene, and varying the thioether carbon chain length from (a) ethyl sulfide, (b) propyl sulfide, (c) butyl sulfide, (d) hexyl sulfide, (e) octyl sulfide, and (f) *n*-dodecyl sulfide. As shown, narrower size distributions are obtained with octyl and *n*-dodecyl sulfides.

Catalytic Reactions of Immobilized Pd Nanoparticles. Soluble colloidal nanoparticles present unique opportunities for homogeneous catalysis because of better activity and selectivity.[17] The 1.7, 2.5, and 3.5 nm Pd nanoparticles were examined by TEM following the first catalytic cycle toward the hydrogenation of styrene → 1-ethylenebenzene. In each case, the Pd nanoparticles were found to aggregate, with the smaller 1.7 nm Pd nanoparticles forming larger sized aggregates, relative to the larger 2.5 and 3.5 nm Pd nanoparticles. Both the 2.5 and 3.5 nm Pd nanoparticles had similar sized aggregates following one catalytic cycle. After the first catalytic cycle, the average reaction yield for the

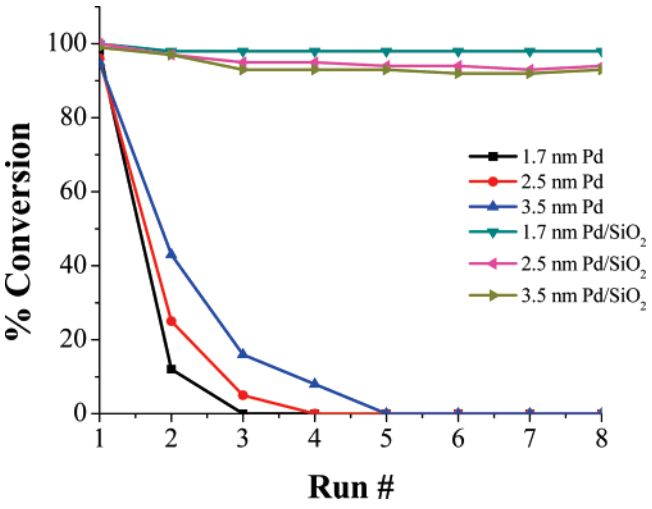

Figure 6. Plots of percent conversion vs number of catalytic cycles for the conversion of styrene to 1-ethylbenzene compared for colloidal and SiO_2 immobilized 1.7, 2.5, and 3.5 nm Pd nanoparticles. In the case of the colloidal particles, the larger the size, the more reusable the catalyst is. When immobilized on SiO_2, the conversion efficiencies are highly improved compared to their colloidal counterparts, however, the smaller the particle size, the better the conversion efficiency.

1.7, 2.5, and 3.5 nm Pd nanoparticles were 98%, 96%, and 95%, respectively. In the second catalytic cycle, the reaction yields decreased to 12%, 25%, and 43%, respectively, and continued to decrease with additional cycles, as shown in Figure 6. The 1.7 nm Pd nanoparticles showed no catalytic activity following two cycles. However, as the data in Figure 6 reveal, we found that the reactivity of the Pd nanoparticles increased with increase in Pd nanoparticle size. This is in contrast to what one would expect, that is, the reactivity would be expected to decrease with increase in particle size because of smaller particles having a greater percentage of their atoms on the particle surface relative to the larger particles. This observation has also been reported by others.[18−20] In addition to loss in catalytic activity of the homogeneous Pd nanoparticles, particle recovery proved to be problematic. Narayanan and El-Sayed have also repeatedly shown that palladium nanoparticles (less than 5 nm) cannot be easily recovered following one catalytic reaction.[17b] Others[21] have shown that a disadvantage to homogeneous metal nanoparticle catalysts is the challenge in their recovery.

Metal nanoparticle immobilization onto solid supports is an attractive approach that has been widely used by several groups.[22] The advantage to this approach is that the activity of the Pd nanoparticles can be utilized while allowing the system to behave heterogeneously. In this regard, we immobilized the *n*-dodecyl sulfide stabilized 3.5 nm Pd nanoparticles onto commercially available and partially dehydrated silica gel, as described in the Experimental Section and as shown in Figure 7. Although the mode of binding between SiO_2 and the immobilized 3.5 nm Pd nanoparticles has not been fully investigated, the Pd/SiO_2 catalysts were stable, selective, and recoverable in the hydrogenation of olefins such as styrene, 1,5-cyclooctadiene, and 6-bromo-1-hexene.

Pd/SiO_2 (0.012 mmol) and styrene (17.40 mmol) were allowed to react in benzene solvent in the presence of hydrogen (∼1 atm) at room temperature for 1 h and were found to produce ethylbenzene in 100% yield, as determined by GC-MS. The experiment could be repeated up to five times by using the same immobilized Pd catalyst to give 1-ethylbenzene quantitatively. Similarly, Pd/SiO_2 catalyzed the hydrogenation of 1,5-cyclooctadiene. GC-MS analysis showed that after 24 h both 1-cyclooctene and cyclooctane had formed in approximately a 1:1 ratio. After 48 h, 1-cyclooctane was found to be the main product. The experiment was repeated using the same catalyst eight times, and in each case, the same product distribution was observed, indicating efficient catalyst recovery.

Hydrogenation of 6-bromo-1-hexene catalyzed by Pd/SiO_2 was examined. Analysis of an aliquot of the reaction mixture obtained after 45 min showed the formation of 1-bromohexane as a major product (∼90%) along with unreacted 6-bromo-1-hexene (∼10%). After 3 h, 1-bromohexane was the sole product and the catalyst could be further reused up to eight times with no measurable loss of activity.

The catalytic activity of 1.7 ± 0.2 nm, 2.5 nm ± 0.1 nm, and 3.5 ± 0.1 nm Pd nanoparticles immobilized on the SiO_2 (Pd/SiO_2) was examined for styrene hydrogenation and was compared to the catalytic activity of the non-immobilized Pd nanoparticles. As shown in Figure 6, all three sizes of Pd/SiO_2 showed no loss in catalytic activity after eight reaction cycles. In addition, the 1.7 nm Pd/SiO_2 showed consistent improved conversion rates (∼99%) compared to the larger 3.5 nm Pd/SiO_2 which had conversion rates of ∼94%. The results demonstrate that surface immobilization prevents particle aggregation and maintains the particles' catalytic efficiency.

Our thioether-stabilized Pd nanoparticles have thus proven to be highly selective toward hydrogenation across C−C double bonds. Most importantly, the hydrogenation of 6-bromo-1-hexene to yield 6-bromohexane, with no destruction of the C−Br bond, indicates the selectivity of the Pd nanoparticles. This is extremely attractive since most C−Br bonds are quite labile.

A common problem often encountered by such heterogeneous catalysts is extensive leaching of the active metal during reactions, which in turn, leads to gradual loss

(17) (a) Roucoux, A.; Schulz, J.; Patin, H. *Chem. Rev.* **2002**, *102*, 3757−3778 and references therein. (b) Narayanan, R.; El-Sayed, M. A. *J. Am. Chem. Soc.* **2003**, *125*, 8340−8347. (c) Collier, P. J.; Iggo, J. A.; Whyman, R. *J. Mol. Catal. A.: Chem.* **1997**, *118*, 145−151. (d) Sculz, J.; Roucoux, A.; Patin, H. *Chem. Eur. J.* **2000**, *6*, 618−624. (e) Chechik, V.; Crooks, R. M. *J. Am. Chem. Soc.* **2000**, *122*, 1243−1244.
(18) Schlogl, R.; Abd Hamid, S. B. *Angew. Chem., Int. Ed.* **2004**, *43*, 1628−1637.
(19) Niu, Y.; Yeung, L. K.; Crooks, R. M. *J. Am. Chem. Soc.* **2001**, *123*, 6840−6846.
(20) Scott, R. W.; Wilson, O. M.; Oh, S.-K.; Kenik, E. A.; Crooks, R. M. *J. Am. Chem. Soc.* **2001**, *123*, 15583−15591.
(21) Kim, S.-W.; Kim, M.; Lee, W. H.; Hyeon, T. *J. Am. Chem. Soc.* **2002**, *124*, 7642−7643.
(22) (a) Galow, T. H.; Drechsler, U.; Hansom, J. A.; Rotello, V. M. *Chem. Commun.* **2002**, 1076−1077. (b) Yuranov, I.; Moeckli, P.; Suvorova, E.; Buffat, P.; Kiwi-Minsker, L.; Renken, A. *J. Mol. Catal. A* **2003**, *192*, 239−251. (c) Bowker, M.; Stone, P.; Morrall, P.; Smith, R.; Bennett, R.; Perkins, N.; Kvon, R.; Pang, C.; Fourre, E.; Hall, M. *J. Catal.* **2005**, *234*, 172−181.

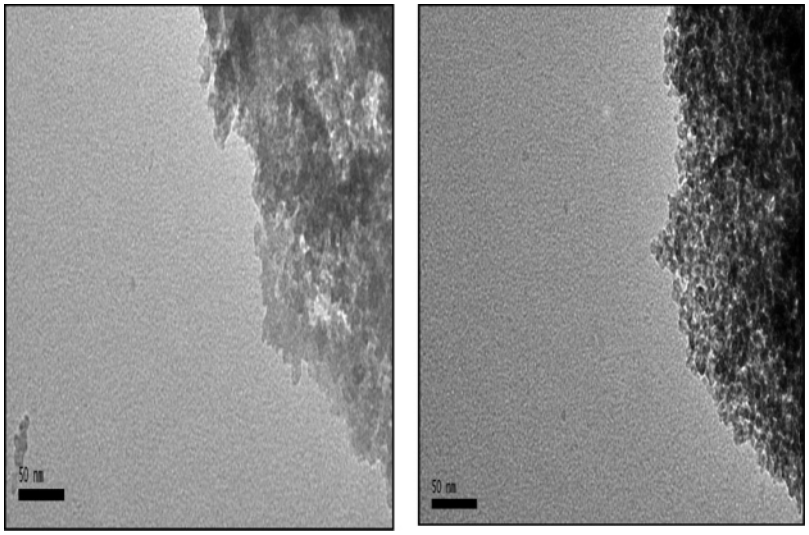

Figure 7. TEM image of (a) calcinated silica gel and (b) Pd immobilized on the silica gel, obtained after the treatment of *n*-dodecyl sulfide stabilized Pd nanoparticles in toluene at room temperature. Scale bar = 50 nm.

in catalytic activity. Our catalysts maintained their catalytic activity and showed no measurable loss after eight recycles.

Conclusion

In summary, a one-step procedure for the gram-scale synthesis of monodisperse palladium nanoparticles with sizes ranging from 1.7 to 3.5 nm has been established. The remarkable feature is that *n*-dodecyl sulfide produces monodisperse Pd nanoparticles regardless of the synthetic procedure used (i.e., pyrolysis, polyol reduction, or chemical reduction). The lack of requirement for a size selection process following the reaction and the cost effectiveness of commercial thioethers are remarkable aspects and clearly show the advantages of the new procedure.

Acknowledgment. We gratefully acknowledge the National Science Foundation (Grant 0548074), Western Michigan University, and the Western Michigan University Faculty Research and Creative Activities Support Fund (FRACASF) Award for financial support of this work.

Note Added after ASAP Publication. The Supporting Information was missing in the version published ASAP June 7, 2007. The corrected version was published ASAP June 20, 2007.

Supporting Information Available: Experimental details and Figures S1−S8. This material is available free of charge via the internet at http://pubs.acs.org.

CM062655Q